

## The Effect of Sulphur (S) Doping and K<sup>+</sup> Adsorption To The Electronic Properties Of Graphene: A Study By DFTB Method

Yuniawan Hidayat\*, Fitria Rahmawati, Eddy Heraldy, Khoirina D Nugrahaningtyas, IF Nurcahyo  
Chemistry Department, Sebelas Maret University, Surakarta, Indonesia

Corresponding Author:  
Yuniawan Hidayat  
yuniawan.hidayat@staff.uns.ac.id

Received: November 2021  
Accepted: March 2022  
Published: September 2022

©Yuniawan Hidayat et al. This is an open-access article distributed under the terms of the Creative Commons Attribution License, which permits unrestricted use, distribution, and reproduction in any medium, provided the original author and source are credited.

### Abstract

A study on the effect of S doping and K<sup>+</sup> adsorption on the electronic properties of graphene has been conducted by DFTB (Density Functional Tight Binding) calculation. The supercell of 40 x 40 x 1 configured from the 4x4x1 unit cell of graphene was optimized. The calculation shows that the Fermi level of graphene shifted from -4.67 eV to -3.57 eV after S doping. In addition, the S presence caused the formation of the gap within the Dirac K of the valence band and conduction band. Meanwhile, K<sup>+</sup> charge distribution has dominantly occurred within the S-graphene than the graphene.

**Keywords:** *DFTB, Graphene, S-Graphene, DOS, Bandgap*

### Introduction

Charge density and charge distribution within a Carbon, C, the atom in a graphene compound will be changed, because of the presence of dopant which induces the 'activation zone' of the graphene surface<sup>[1]</sup>. Doping of the Sulphur atom can increase the number of free-valence electrons and then allow the electronic conductivity and chemical reactivity to increase<sup>[2]</sup>. The reactivity zone may shift the Fermi level to above the Dirac point, and the Density of State, DOS near the Fermi level can be reduced<sup>[3],[4]</sup> allowing the opening gap between the conduction band and valence band. Such kind of an active zone can be increased by submitting a dopant such as a Sulphur atom<sup>[5],[6]</sup>.

Graphene consists of sp<sup>2</sup> carbon, in which every C atom has s, p<sub>x</sub>, and p<sub>y</sub> orbitals developing three σ bonding with the nearest atoms. The overlap of p<sub>z</sub> orbital within each C atom and

the nearest C atom causes π orbitals (valence band) to be filled with electrons and the π\* orbitals (the conduction band) to be empty. The valence and conduction band are located in corner of the Brillouin zone which leads the band gap to become narrower and close to zero<sup>[7]</sup>. The S doped-graphene is known to have a graphitic bonding, in which the S atom that replaces the C atom of the graphene forms a graphitic bonding with the three- nearest C atoms by the σ bonding<sup>[8]</sup>.

Meanwhile, the interaction between alkali ion and graphene is influenced by the active surface of graphene found from doping with a non-carbon element, such as Sulphur. The physical adsorption of the metal element to graphene, and the charge-transfer to metal or charge-transfer from metal to graphene cause the Fermi level to shift. The work function, W of the metal element on the graphene surface is determined by the Fermi level position ( $W_f = -E_f$ )<sup>[9]-[12]</sup>.

It is known that DFTB can calculate a large electronic system which hard to is conducted by a conventional *ab initio* method<sup>[13]</sup>. Previous research has successfully calculated the electronic properties of molecules to predict chemical activity in solid, supramolecular, and carbon<sup>[14]–[17]</sup>. A calculation of adsorption modeling of Ni-pyridine on a graphene surface found the calculated adsorption energy by DFTB and DFT were distinguished by only 1 kcal/mol. It proves the precise calculation of DFTB with a faster calculation compared to DFT<sup>[18]</sup>. For example, the electronic structure and stretching effect of porous graphene and nanotube graphenylene were also can be studied by DFTB. The result shows a large band gap with an energy of 3.3 eV. Meanwhile, a nanotube graphenylene has a band gap energy of 0.7 eV<sup>[19]</sup>.

This article discusses the relation between S doping into graphene with the DOS change, the Fermi level shift, and the structure of the conduction band. Those three parameters inform the prediction of S-doped-graphene performance to the K<sup>+</sup> adsorption. The performance was then compared with the undoped graphene.

## Experimental

### Materials

The structure materials for computational models are pristine graphene, S-doped graphene, pristine graphene with K<sup>+</sup> ion, and S-doped graphene with K<sup>+</sup> ion. All the structures are modified from the graphite unit cell of Kristin Person's material data<sup>[20]</sup>.

### Instruments

The software consists of the DFTB+ package program<sup>[21]</sup>, VESTA (Visualization for Electronic and Structural Analysis) program<sup>[22]</sup>, and the AMS (Amsterdam Modeling Suite)<sup>[23]</sup>. Hardware is a standalone personal computer with the main specification of core processor Intel i7 @3600 MHz, 256 GB SSD, and 8 GB RDRAM3.

## Method

The Kohn-Sham DFT equation may be converted to the DFTB equation using the Taylor series expansion. By expanding the exchange-correlation energy functional to the second order, the total energy may be expressed as the following equation<sup>[24]</sup>.

$$E_{\text{DFTB3}}[Q(r)] = \frac{1}{2} \sum_{ab} \frac{z_a z_b}{R_{ab}} - \frac{1}{2} \iint \frac{Q^0(r^0) Q^0(r')}{|r-r'|} dr dr' - \int V^{xc}[Q^0] Q^0(r) dr +$$

$$E^{xc}[Q^0] + \sum_i n_i \langle \psi_i | \hat{H}[Q^0] | \psi_i \rangle +$$

$$\frac{1}{2} \iint \left( \frac{1}{|r-r'|} + \frac{\delta^2 E^{xc}[Q]}{\delta Q(r) \delta Q(r')} \Big|_{Q^0} \right) \delta Q(r) \delta Q(r') dr dr' +$$

$$\frac{1}{6} \iiint \frac{\delta^3 E^{xc}[Q]}{\delta Q(r) \delta Q(r') \delta Q(r'')} \Big|_{Q^0} \delta Q(r) \delta Q(r') \delta Q(r'') dr dr' dr'' \quad (1)$$

Notation  $Z_a$  and  $Z_b$  refer to the effective charge of atoms  $a$  and  $b$  separate along the  $R$  distance. The  $\rho(r)$  is the electron density as a function with  $r$  (electron distance) which is fluctuated by density fluctuation of the reference electron density or  $\rho$ . The  $V^{xc}$  and  $E^{xc}$  correspond to the potential and energy of the exchange-correlation function. The  $n_i$  refers to the occupancy number of Kohn-Sham orbital  $i$  and the  $\psi_i$  is a wavefunction of  $i$ .

The SCC-DFTB is a self-consistent-charge method, regarding the second or three-order expansion of the energy around a reference density as appearing in the sixth and seventh terms in equation 1. The second order denotes the interaction of the system charges, while the third order denotes the chemical hardness of the atoms as a result of the charges' interaction. The full set of equation 1 with the third order included is called the DFTB3, while if the equation ends with the second order term is called DFTB2. SCC-DFTB is well suited to studying the electrical properties of systems due to the charge interactions incorporated in the calculations.

The Crystal parameters of graphene were taken from Kristin Person, 2014<sup>[20]</sup>. The properties of

the original unit cell have parameters as follows: The lattice of  $a$ ,  $b$ , and  $c$  correspond to 2.468 Å, 2.468 Å and 8.685 Å with  $\alpha$ ,  $\beta$ , and  $\gamma$  are correspond to 90°, 90° and 120°. The lattice coordinate of  $a$ ,  $b$ , and  $c$  of four C atoms are 0, 0,  $\frac{3}{4}$ ; 0, 0,  $\frac{1}{4}$ ;  $\frac{1}{3}$ ,  $\frac{2}{3}$ ,  $\frac{3}{4}$ ; and  $\frac{2}{3}$ ,  $\frac{1}{3}$ ,  $\frac{1}{4}$ . The crystal system follows the hexagonal with a point group of 6/mmm. The unit cell then modifies to 4x4x1 by VESTA as a new unit cell. For sampling, the supercell of 40 x 40 x1 was optimized. The optimization used SCC (self-consistent charges)- DFTB method with the p-orbital defined as the maximum angular momentum for each atom. The Slater-Koster parameter of mio-1-1 was implemented except for the S atom treated by 3ob-3-1. The orbitals were a threat with the fermi occupation method at around 0 K. The K-points of Brillouin zone was setting up as  $\Gamma$  (0.0 0.0 0.0), M (0.5 0.0 0.0) and K (0.3333 0.333 0.0). Similar steps of optimization were then conducted for graphene and S-graphene in interaction with  $K^+$ . The calculation was conducted by calculating the engine of DFTB+. The optimized structure was then recalculated using AMS to generate the IR spectra.

The density of state (DOS), atomic charges, and the band energy structure of each model were taken from the calculation. The band structures and Fermi level was extracted from the optimized-state calculation. The DOS graphic and the structure of the band were then set up into Fermi level = 0 which was found from  $E_0$  –

$E_f$ . The  $E_0$  is the Fermi level of 0 eV and  $E_f$  is the calculated-Fermi level. The work of electronic function ( $W_f$ ) of the graphene was calculated based on the Fermi shifting and it was formulated as (equation 2)<sup>[9]-[12]</sup>.

$$W_f = -E_f \quad (2)$$

## Results and Discussion

The crystal lattice of Graphene and S-graphene were firstly optimized along the  $a$  and  $b$  vector directions. The results for both graphene and S-graphene are described in Figure 1. The optimum calculation of graphene crystal lattice found the closest C-C distance as 1.428 Å. The distance is in agreement with the computational modeling of the previous research on graphene and graphite using ab initio and DFT<sup>[8],[25]-[27]</sup>.

The presence of S in the graphene structure changes the C-C distance to be between 1.402 Å – 1.467 Å. The change of distance was caused by the reduction of the symmetry level of graphene due to S doping. The SSC-DFTB calculation found that the distance of C-S is 1.69 Å which is below the result of the DFT calculation i.e., 1.76 – 1.78 Å<sup>[28],[29]</sup>. The optimum distance of  $K^+$  from the surface of graphene is 2.77 Å, and it is 2.94 Å from the S-graphene surface. A DFT calculation also finds a distance between  $K^+$  ions to the surface of graphene as 2.6 – 2.7 Å<sup>[30],[31]</sup>.

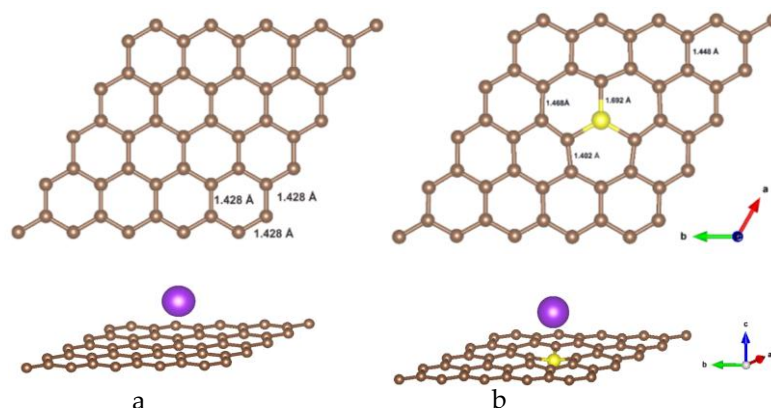


**Figure 1.** The 4x4x1 unit cell of (a) pure graphene and K/graphene, and (b) S-graphene and K/S-graphene. Brown, yellow, and magenta correspond to carbon, sulfur, and potassium ion, respectively

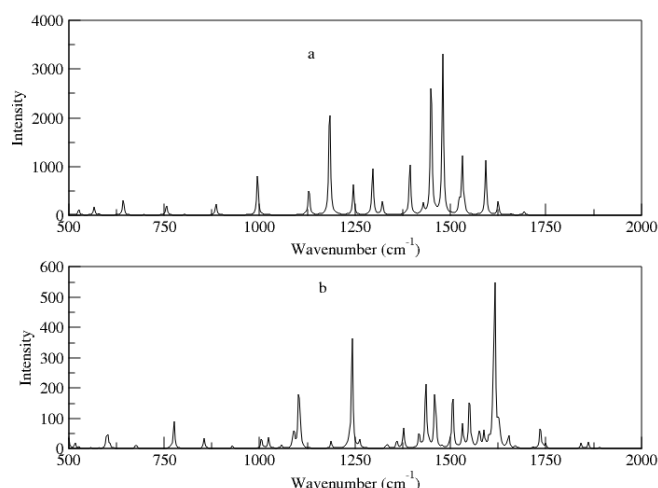


**Figure 2.** The wavenumber vibration of (a) Pure graphene and (b) S-graphene

The vibration of the pristine graphene and S-graphene is depicted in Figure 2. The wavenumber between 1200 and 1300  $\text{cm}^{-1}$  is specific for D band vibration, while around 1500  $\text{cm}^{-1}$  indicating for G band vibration<sup>[32],[33]</sup>. The DFTB results are less accurate in determining the G band vibration, as shown in Figure 2a, the G bands show a lower wavenumber. The band shift of both bands to the higher wavenumber is well predicted by the method, corresponding to the change of the symmetrical degree around the S-doped of graphene (Figure 2b).

The Fermi level of the pure graphene was found to be 4.6672 eV, which is in agreement with the other experiment on the Fermi level calculation which lies between 4.2 – 4.8 eV<sup>[9],[32],[34]</sup>. Sulfur doping shifted the Fermi level energy at -1.0903 eV to become 3.5679 eV. Fig. 3(a) shows the DOS shifting after the Fermi level for both structures which was set to zero point. The presence of sulfur is responsible for the left shift of the DOS graphene and the rise of the intensity at around Fermi. It indicates the presence of an electronic state because of the injection of sulfur electrons into the graphene structure.

The  $\text{K}^+$  ion shifted the Fermi level of graphene and S-graphene into 2.0866 eV and -2.0312 eV, respectively. Fig 3(b) describes the DOS of graphene and S-graphene that interact with  $\text{K}^+$

ions and cause the Fermi level to undergo left shifting. The negative shifting indicates the presence of charge transfer of  $\text{K}^+$  ion into graphene structure<sup>[35]</sup>. The  $\text{K}^+$  presence increases DOS intensity around the Fermi level of graphene, indicating the increase of the electronic state on the Fermi level. A similar electronic state appears on the S-graphene; however, the increase was distributed averagely to the DOS, leading to a homogeneous intensity of fluctuation within the Fermi area.

Charge transfer phenomena were confirmed by the change of atomic charge at around dopant and  $\text{K}^+$  before and after the interaction. Table 1 shows in detail the result of the gross-charge calculation of each atom. The C atom that was investigated before and after interaction with  $\text{K}^+$  is the same whether for graphene or S-graphene. The C atom in graphene structure is signed by  $\text{C}_{(\text{graphene})}$  having neutral or zero charge. Meanwhile, after S doping the  $\text{C}_{(\text{S-graphene})}$  became negatively charged. The charge is -0.0000986e, which seems to be too small because the charge which is transferred from sulfur was distributed averagely on the graphene surface. After the interaction with  $\text{K}^+$ , the charge of the C atom whether in the graphene structure or S-graphene became more negative, indicating for accepting electron charge from  $\text{K}^+$ . The positive charge of  $\text{K}^+$  decreases after interaction because

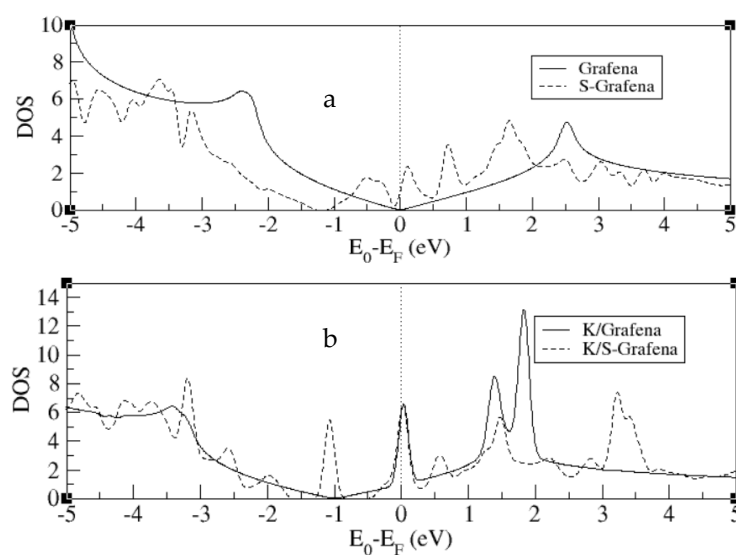


**Figure 3.** DOS after the Fermi level was set up into zero from (a) graphene and S-graphene, and b) K/graphene and K/S-graphene

**Table 1.** The gross charges ( $e$ ) of corresponding atoms

Atom	Before interaction with $K^+$	After interaction with $K^+$
C(Graphene)	0.0000	-0.0319
C(S-Graphene)	-0.000986	-0.0182
S(S-Graphene)	0.5130	0.3590
K(Graphene)	1.0000	0.7840
K(S-Graphene)	1.0000	0.7120

the charge was transferred to the graphene. After interaction with  $K^+$ , the charge of the C atom is more negative i.e.,  $-0.0319e$ , than the C charge on the S-graphene, which is  $-0.0182e$ . It seems that the graphene structure is easier to receive charge transfer from  $K^+$ . However, this is not correct because the  $K^+$  charge was reduced by  $0.228e$  during interaction with S-graphene, and it was reduced by  $0.216e$  during interaction with graphene.

The charge transfer from  $K^+$  ion to S-graphene was more occurred than to graphene. With the S dopant, the C graphene around the doping area can accommodate more charge. Table 1 shows the S charge was significantly reduced by accepting electron charge from  $K^+$ . It confirms that the charge transfer of the  $K^+$  ion is dominant with the presence of sulphur in the graphene.

The structure of band energy for graphene, S-graphene, K/Graphene, and K/S-graphene are described in Fig.4. Index  $\Gamma$ , M and K are the high symmetry points on the Brillouin zone of the crystal system, especially of the graphene which has a hexagonal lattice. The energy band of graphene as depicted in Fig. 4(a), shows a stacking point of K as the 'direct cone' of graphene. The presence of S dopant which replaced a C atom significantly changes the energy band by decreasing the Fermi level position and opening a band gap at the Direct K point (Fig. 4b). The formation of a bad gap due to S doping is exactly in agreement with a prediction by DFT calculation<sup>[36],[37]</sup>. The band gap energy of  $0.38$  eV was lower than the DTF result ( $0.57$  eV)<sup>[35]</sup>.

The presence of  $K^+$  ion on the surface with the position above the graphene ring would not

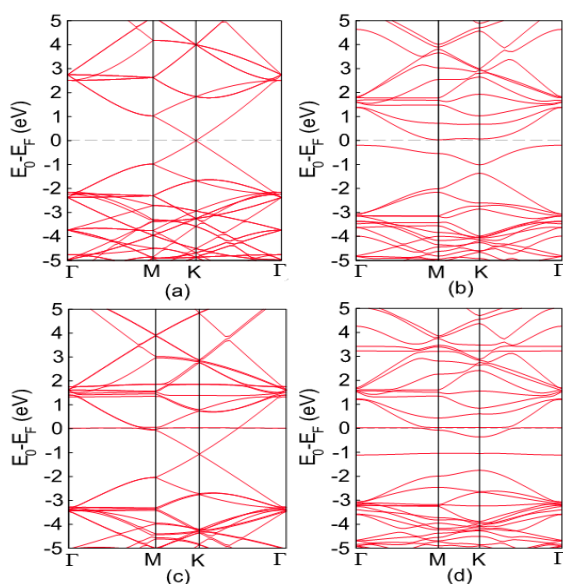


**Figure 4.** Structure of the band energy of (a) graphene, (b) S-Graphene, (c) K/Graphene, and (d) K/S-Graphene

produce gap energy, but decreased the DOS of graphene below Fermi Level (Fig. 4c), in line with the experimental prediction<sup>[38]</sup>. Meanwhile, in an S doped-graphene, the interaction with the  $K^+$  ion on the surface caused the formation of larger gap energy (0.67 eV). Fig. 4d depicts the larger gap energy appearing due to the presence of  $K^+$  ions on the S-graphene surface. By exposing the 'direct cone' through gap energy, therefore graphene will have a better electronic conductivity<sup>[39]</sup>.

The performance of electronic conductivity correlates with the electrostatic potential of a system. The electronic performance of graphene which is formulated as  $W_f = E_f$  can be defined as the energy needed to move the electrons from the Fermi level to the vacuum level<sup>[10]</sup>. The functional energy of graphene, S-graphene, K/graphene, and K/S graphene is 4.67 eV, 3.57 eV, 2.09 eV, and 2.03 eV, respectively. The values show that electron movement within the graphene structure is easier to occur by the presence of S dopant and the interaction with the  $K^+$  ion.

### Conclusions

The DFTB method can be used to investigate the electronic properties of graphene, in which the calculation results are close to the

calculation made by the DFT method. The electron movements in graphene structure increase by the presence of S dopant and the interaction with  $K^+$  ion. It is proven by the Fermi level shifting to a lower state, the higher charge transfer occurs, and the presence of gap energy on the structure of band energy. The values of functional electronic works confirm well the conclusion

### Acknowledgments

The author would like to acknowledge the Sebelas Maret University for supporting this work through the Riset Groups Grant of the NON-PNBP Funding.

### References

1. Zhang, L. & Xia, Z., Mechanisms of Oxygen Reduction Reaction on Nitrogen-Doped Graphene for Fuel Cells. *J. Phys. Chem. C*, **115(22)**: 11170–11176 (2011).
2. Feng, L., Qin, Z., Huang, Y., Peng, K., Wang, F., Yan, Y. & Chen, Y., Boron-, sulfur-, and phosphorus-doped graphene for environmental applications. *Sci. Total Environ.*, **698**: 134239 (2020).
3. Ketabi, N., de Boer, T., Karakaya, M., Zhu, J., Podila, R., Rao, A. M., Kurmaev, E. Z., et

- al.*, Tuning the electronic structure of graphene through nitrogen doping: experiment and theory. *RSC Adv.*, **6(61)**: 56721–56727 (2016).
- Joucken, F., Tison, Y., Le Fèvre, P., Tejada, A., Taleb-Ibrahimi, A., Conrad, E., Repain, V., *et al.*, Charge transfer and electronic doping in nitrogen-doped graphene. *Sci. Rep.*, **5(1)**: 14564 (2015).
  - Li, Y., Wang, G., Wei, T., Fan, Z. & Yan, P., Nitrogen, and sulfur co-doped porous carbon nanosheets derived from willow catkin for supercapacitors. *Nano Energy*, **19**: 165–175 (2016).
  - Qie, L., Chen, W. M., Wang, Z. H., Shao, Q. G., Li, X., Yuan, L. X., Hu, X. L., *et al.*, Nitrogen-doped porous carbon nanofiber webs as anodes for lithium-ion batteries with a superhigh capacity and rate capability. *Adv. Mater.*, **24(15)**: 2047–2050 (2012).
  - Luo, Z., Lim, S., Tian, Z., Shang, J., Lai, L., MacDonald, B., Fu, C., *et al.*, Pyridinic N doped graphene: synthesis, electronic structure, and electrocatalytic property. *J. Mater. Chem.*, **21(22)**: 8038 (2011).
  - Lu, Z., Li, S., Liu, C., He, C., Yang, X., Ma, D., Xu, G., *et al.*, Sulfur doped graphene as a promising metal-free electrocatalyst for oxygen reduction reaction: a DFT-D study. *RSC Adv.*, **7(33)**: 20398–20405 (2017).
  - Yang, N., Yang, D., Chen, L., Liu, D., Cai, M. & Fan, X., Design and adjustment of the graphene work function via size, modification, defects, and doping: a first-principle theory study. *Nanoscale Res. Lett.*, **12(1)**: (2017).
  - Gholizadeh, R. & Yu, Y. X., Work functions of pristine and heteroatom-doped graphenes under different external electric fields: An ab initio DFT study. *J. Phys. Chem. C*, **118(48)**: 28274–28282 (2014).
  - Ooi, N., Rairkar, A. & Adams, J. B., Density functional study of graphite bulk and surface properties. *Carbon N. Y.*, **44(2)**: 231–242 (2006).
  - Khomiyakov, P. A., Giovannetti, G., Rusu, P. C., Brocks, G., Van Den Brink, J. & Kelly, P. J., First-principles study of the interaction and charge transfer between graphene and metals. *Phys. Rev. B - Condens. Matter Mater. Phys.*, **79(19)**: 1–12 (2009).
  - Spiegelman, F., Tarrat, N., Cuny, J., Dontot, L., Posenitskiy, E., Martí, C., Simon, A., *et al.*, Density-functional tight-binding: basic concepts and applications to molecules and clusters. *Adv. Phys. X*, **5(1)**: 1710252 (2020).
  - Poh, C.-K. & Shieh, H.-P. D., Density Functional Based Tight Binding (DFTB) Study on the Thermal Evolution of Amorphous Carbon. *Graphene*, **05(02)**: 51–54 (2016).
  - Zhang, Q., Khetan, A. & Er, S., Comparison of computational chemistry methods for the discovery of quinone-based electroactive compounds for energy storage. *Sci. Rep.*, **10(1)**: 22149 (2020).
  - Sengupta, S., Murmu, M., Murmu, N. C. & Banerjee, P., Adsorption of redox-active Schiff bases and corrosion inhibiting property for mild steel in 1 molL<sup>-1</sup> H<sub>2</sub>SO<sub>4</sub>: Experimental analysis supported by ab initio DFT, DFTB, and molecular dynamics simulation approach. *J. Mol. Liq.*, **326**: 115215 (2021).
  - Selli, D., Fazio, G. & Di Valentin, C., Modelling realistic TiO<sub>2</sub> nanospheres: A benchmark study of SCC-DFTB against hybrid DFT. *J. Chem. Phys.*, **147(16)**: 164701 (2017).
  - Kanematsu, Y., Gohara, K., Yamada, H. & Takano, Y., Applicability of Density Functional Tight Binding Method with Dispersion Correction to Investigate the Adsorption of Porphyrin/Porphycene Metal Complexes on Graphene. *Chem. Lett.*, **46(1)**: 51–52 (2017).
  - Fabris, G. S. L., Junkermeier, C. E. & Paupitz, R., Porous graphene, and graphenylene nanotubes: Electronic structure and strain effects. *Comput. Mater. Sci.*, **140**: 344–355 (2017).
  - Persson, K., Materials Data on C (SG:194) by Materials Project. (2014).

- doi:10.17188/1208406
21. Hourahine, B., Aradi, B., Blum, V., Bonafé, F., Buccheri, A., Camacho, C., Cevallos, C., *et al.*, DFTB+, a software package for efficient approximate density functional theory based atomistic simulations. *J. Chem. Phys.*, **152(12)**: 124101 (2020).
  22. Momma, K. & Izumi, F., VESTA : a three-dimensional visualization system for electronic and structural analysis. *J. Appl. Crystallogr.*, **41(3)**: 653–658 (2008).
  23. R. Rüger, A. Yakovlev, P. Philippsen, S. Borini, P. Melix, A.F. Oliveira, M. Franchini, T. van Vuren, T. Soini, M. de Reus, M. Ghorbani Asl, T. Q. Teodoro, D. McCormack, S. Patchkovskii, T. H., AMS DFTB. (2021).
  24. Elstner, M. & Seifert, G., Density functional tight binding. *Philos. Trans. R. Soc. A Math. Phys. Eng. Sci.*, **372(2011)**: 20120483 (2014).
  25. Wang, J., Ma, F. & Sun, M., Graphene, hexagonal boron nitride, and their heterostructures: properties and applications. *RSC Adv.*, **7(27)**: 16801–16822 (2017).
  26. Ngoc Thanh Thuy, T., Lin, S.-Y., Lin, C.-Y. & Lin, M.-F., *Geometric and Electronic Properties of Graphene-Related Systems*. CRC Press, (2017). doi:10.1201/b22450
  27. Tran, N. T. T., Lin, S.-Y., Lin, C.-Y. & Lin, M.-F., Geometric and electronic properties of graphene-related systems: Chemical bondings. *Graphene*, **05(02)**: 35–38 (2017).
  28. Zhang, Q., Wang, B. X., Yu, Y. B., Chen, B.-Y. & Hong, J., Sulfur doped-graphene for enhanced acetaminophen degradation via electro-catalytic activation: Efficiency and mechanism. *Sci. Total Environ.*, **715**: 136730 (2020).
  29. Denis, P. A., Huelmo, C. P. & Iribarne, F., Theoretical characterization of sulfur and nitrogen dual-doped graphene. *Comput. Theor. Chem.*, **1049**: 13–19 (2014).
  30. Kaneko, T. & Saito, R., First-principles study on the interlayer state in alkali and alkaline earth metal atoms intercalated bilayer graphene. *Surf. Sci.*, **665**: 1–9 (2017).
  31. Peles-Lemli, B., Kánnár, D., Nie, J. C., Li, H. & Kunsági-Máté, S., Some Unexpected Behavior of the Adsorption of Alkali Metal Ions onto the Graphene Surface under the Effect of External Electric Field. *J. Phys. Chem. C*, **117(41)**: 21509–21515 (2013).
  32. Liu, D., He, M., Huang, C., Sun, X. & Gao, B., Fermi-Level Dependence of the Chemical Functionalization of Graphene with Benzoyl Peroxide. *J. Phys. Chem. C*, **121(19)**: 10546–10551 (2017).
  33. Hassani, F., Tavakol, H., Keshavarzipour, F. & Javaheri, A., A simple synthesis of sulfur-doped graphene using sulfur powder by chemical vapor deposition. *RSC Adv.*, **6(32)**: 27158–27163 (2016).
  34. Yuan, J., Dai, J.-Q., Ke, C. & Wei, Z.-C., Interface coupling and charge doping in graphene on ferroelectric BiAlO<sub>3</sub> (0001) polar surfaces. *Phys. Chem. Chem. Phys.*, **23(5)**: 3407–3416 (2021).
  35. Dimakis, N., Valdez, D., Flor, F. A., Salgado, A., Adjibi, K., Vargas, S. & Saenz, J., Density functional theory calculations on alkali and the alkaline Ca atoms adsorbed on graphene monolayers. *Appl. Surf. Sci.*, **413**: 197–208 (2017).
  36. Denis, P. A., Band gap opening of monolayer and bilayer graphene doped with aluminium, silicon, phosphorus, and sulfur. *Chem. Phys. Lett.*, **492(4–6)**: 251–257 (2010).
  37. Denis, P. A., Concentration dependence of the band gaps of phosphorus and sulfur-doped graphene. *Comput. Mater. Sci.*, **67**: 203–206 (2013).
  38. Nigar, S., Zhou, Z., Wang, H. & Imtiaz, M., Modulating the electronic and magnetic properties of graphene. *RSC Adv.*, **7(81)**: 51546–51580 (2017).
  39. Iyakutti, K., Kumar, E. M., Lakshmi, I., Thapa, R., Rajeswarapalanichamy, R., Surya, V. J. & Kawazoe, Y., Effect of surface doping on the band structure of graphene: a DFT study. *J. Mater. Sci. Mater. Electron.*, **27(3)**: 2728–2740 (2016).